inter-noise 2009
innovations in practical noise control
2009 August 23-26
Ottawa, Canada

Gear noise: anatomy, prediction and solutions

Rajendra Singh[1]
Acoustics and Dynamics Laboratory
Department of Mechanical Engineering
The Ohio State University
Columbus, OH 43210 USA

ABSTRACT

This lecture examines the anatomy of two major gear noise (whine and rattle) problems and identifies their sources. First, typical steady state whine excitations include static transmission error (due to manufacturing inaccuracies and elastic deformations), variations in contact stiffness, sliding friction, force shuttling, etc. Dynamic forces and motions from the whine sources are transmitted to the casing and surrounding structures via structure-borne paths including bearings and then radiated at mesh frequencies and associated side-bands. Whine problems are examined in frequency and order domains over applicable torque loads and rotational speeds. Second, periodic vibro-impacts (gear rattle) under light mean loads are investigated in time or cyclic domain. Torque fluctuations typically excite geared torsional systems (with discontinuous nonlinearities including gear backlashes) and thereby generate high impulsive torsional accelerations, dynamic loads, and sounds. This lecture also discusses predictive tools for gear whine and gear rattle, illustrates sample results, suggests noise control strategies for both problems, identifies a few unresolved issues, and finally recommends some research directions.

1. INTRODUCTION

Gear noise has been a historical problem as evident from the observation made by Earle Buckingham in his landmark book (1949): “it is not a question of why gears are noisy but rather why are they ever quiet.” Gear noise has always been a concern among the designers and manufacturers of various consumer and commercial products such as automobiles, power tools, household appliances, and helicopters. It has a significant influence on the perceived quality and performance of a product by its user in addition to meeting stringent noise regulations and standards in some cases. Accordingly, strategies for gear noise reduction usually focus on reducing objective noise levels as well as improving subjective (sound quality) metrics.

Table 1 provides an overview of two common gear noise problems: gear whine and gear rattle. Sometimes the gear noise term is synonymous with whine as this type of noise is characterized at the gear mesh frequencies and their side bands. Typically whine levels depend on the mean torques (T) and speeds (Ω). Several examples will be considered in this paper to fully illustrate its nature and source-path-receiver characterization. At very low loads, rattle noise is introduced. Vibro-impacts, induced by backlash between meshing gears, lead to excessive vibration, noise, and dynamic loads in many geared rotating systems such as automotive transmissions, machine tools, and appliances. Excessive backlash between gears

[1] Email address: singh.3@osu.edu

could enhance noise by 2 to 14 dB (Mitchell, 1971) while insufficient backlash could create interference problems, and even the lubrication oil could be trapped. The gear rattle problem is more pronounced in essentially unloaded meshes. Therefore, we consider a typical rattle problem in a five-speed manual transmission of a front wheel drive automobile a key example. Further, backlash may also affect the gear whine noise under resonant conditions.

Table 1: An overview of two common gear noise problems

Issue	Whine	Rattle
Nature	• Steady state vibrations of gear pair(s) • Modulated tones (gear mesh frequencies and side bands)	• Backlash-induced single- and double-sided impacts and tooth separations • Cyclic transients
Source(s)	Gear mesh interface primarily (transmission error, mesh stiffness variations, sliding friction, etc.)	Torque pulsations primarily from source (or load)
Mean Torque Load	At all loads, though high noise levels are seen at higher loads	At low or zero mean loads
Key Factors	• Manufacturing errors • Gear contact mechanics • Tooth modification	• Torsional system issues including drag torque and inertial distribution • Interactions among nonlinear elements

Given the vast nature of topics that must be addressed to examine gear whine and rattle problems, only certain issues (of interest to noise control engineers and acousticians) are covered in this lecture. Examples along with some insights will be provided; however, the interested reader is well advised to review the literature cited. The Ohio State University maintains an extensive listing of papers on this topic. According to the latest search, about 800 papers on whine and about 45 papers on rattle are found. Some of them simply mention noise as a key issue. Some of the earlier articles such as by Optiz (1968), Welbourne (1979), and Mitchell (1971) and book chapters such as by Houser (1992, 2007), Smith (1999), Tuma (2007), George (1974), and Mark (1992b) provide overviews mostly on gear whine. Thus, the intent of this article is to provide a primer covering sources, system-oriented mathematical models, and some noise control strategies for both whine and rattle problems.

2. ANATOMY OF GEAR WHINE SOURCES

A. Acoustic Efficiency Type Global Relationships

In a global sense, a geared system or power transmission device itself may be viewed as the noise source and then quantified by its sound power (W) and acoustic radiation efficiency (η_a), where $\eta_a = W/W_{mech}$, where $W_{mech} = T\Omega$ is the mechanical (or mean) power that is being transmitted by the geared system at a given torque (T) and speed (Ω). Based on the overall free field sound pressure level (L_p, dB re 20 μPa) measurements of over 70 gearboxes (Optiz, 1968) over a range of 10 kW to 10 MW mechanical powers, the following relationship emerges:

$$L_p \cong 10\mathrm{Log}_{10}\left(\frac{\eta_a W_{mech}}{10^{-12}}\right) + 10\,\mathrm{Log}_{10}\left(\frac{Q}{4\pi r^2}\right). \quad (1)$$

Here, Q is the source directivity, and r is the distance from the gearbox. Based on the measured data (Optiz, 1968) and curve fits as shown in Figure 1, the following observations can be made. 1. Opitz (1968) classified gears based on their accuracy quality from 'E' (poor quality with $\eta_a \geq 2.5 \times 10^{-6}$) to "A" (accuracy difficult to achieve with $\eta_a \leq 10^{-8}$). 2. A nominal value of $\eta_a = 2 \times 10^{-7}$ seems to fit the mean trend. 3. At a given W_{mech}, the L_p range is about 20 dB. 4. It is difficult to extrapolate this data to lower W_{mech} values as the gear rattle problem might be introduced at reduced loads. 5. Empirical data suggests that a lower limit of L_p may exist even for a highly accurate gear pair, and this implies that it is difficult to design a silent gear pair. 6. A literature search indicates that the lowest value of η_a is about 10^{-9} (as found by Niemann and Boethge (1970) at a specific tooth load).

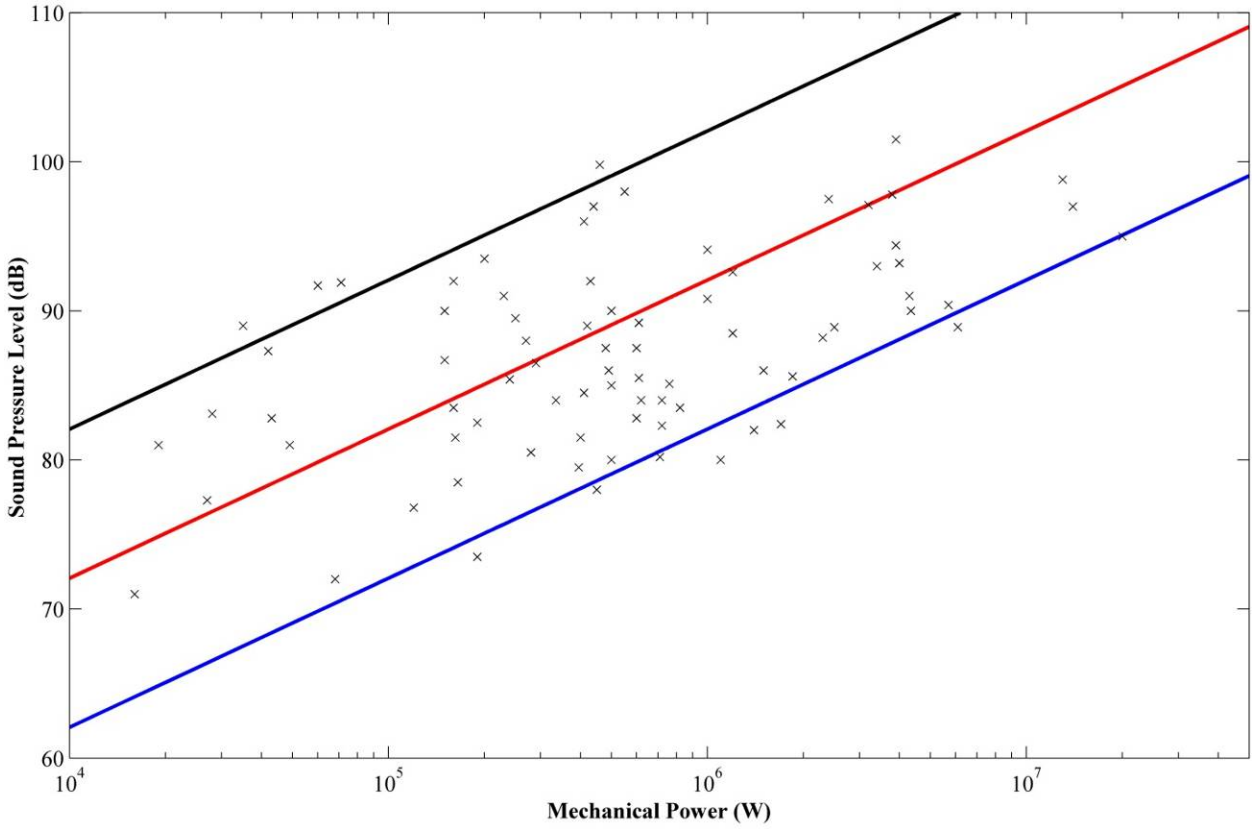

Figure 1: Influence of mechanical power transmitted (W_{mech}) and acoustic efficiency (η_a) on the overall gear (whine) noise levels in terms of L_p (dB re 20 μPa) at r = 4 m. Key: x measured noise data reported by Optiz (1968); — (black) Eq. (1) with $\eta_a = 2 \times 10^{-6}$; — (red) with $\eta_a = 2 \times 10^{-7}$; — (blue) with $\eta_a = 2 \times 10^{-8}$.

B. Gear Mesh Frequencies and Side Bands

Gear whine noise is characterized by the gear mesh or tooth passage frequency (f_m), its harmonics, and the surrounding side bands (due to amplitude, frequency, and phase modulations). Consider a single gear pair where f_{s1} is the input speed (Hz), N_1 is the number of teeth on the input (1) gear, f_{s2} is the output speed (Hz), and N_2 is the number of teeth on the output (2) gear. We should observe the following sets of frequencies:

- Shaft frequencies and their harmonics: if_{s1}; if_{s2} (i = 1, 2, - -)

- Gear mesh frequency and its harmonics: mf_m (m = 1, 2, - -) where $f_m = N_1 f_{s1} = N_2 f_{s2}$
- Side bands: $mf_m \pm if_{s1}$; $mf_m \pm if_{s2}$ (i = 1, 2, - - and m = 1, 2, - -)

In some cases, we might also observe the ghost (or phantom) frequency which is a non-integer multiple of f_m such as πf_m. Also, other periodic phenomena might be captured by the sensors such as qf_{s1} where q is the number of holes in the input gear body. Of course, the spectra under the forced conditions are governed by the sources (and their strengths at f_m, $2f_m$, etc.), system resonances, structure-borne noise paths, and radiation from casing or supporting structures. Since the noise and vibration levels depend on the operating conditions including T, Ω, temperature, etc., waterfall plots over the applicable range(s) are preferred. In a system where the speed varies, order domain (say the orders of f_{s1}) is a better choice to properly display and interpret gear whine signatures (Houser and Singh, 2008; Smith, 1999; Taylor, 2000; Tuma, 2007).

C. Gear Whine Sources

Historically, variations in the static transmission error e(t) and mesh stiffness $k_m(t)$ are viewed as the dominant vibrational sources at the gear mesh interface. These are periodic of the mesh period ($\tau_m = 1/f_m$) though components at the lower frequencies can also be embedded in e(t). The static transmission error (STE) is defined as the deviation from ideal conjugacy and it includes manufacturing effects as well as elastic deformations under a given mean load T (Munro, 1990; Houser, 1992;). Thus the loaded e(t) term is often employed for calculations. One could also define the "static" mesh force $F_{ms}(t) = k_m(t)\, e(t)$, as the source since it includes both e(t) and $k_m(t)$. Sliding fiction force $F_f(t)$ is yet another source that depends on the normal tooth load N(t) and the coefficient of friction μ. Note that the sliding action changes direction at the pitch point. Yet other sources of whine noise include uneven load distributions on the teeth (force shuttling), backlash-induced tooth impacts, and in some cases, aerodynamic sources at very high speeds.

In addition to the above mentioned sources, the internal gear system itself acts as the source regime (in addition to acting as the key the structural path). Thus, torsional-fluctural resonances of the gear pair(s), shafts, bearings, and torsional dynamics of the drive system including motor and load affect the interfacial conditions and generate dynamic transmission error $\delta(t)$ and dynamic mesh force $F_{md}(t) = k_m\delta(t) + c_m\dot{\delta}(t)$ using a linear time-invariant model where c_m is the mesh damping coefficient. Note that $k_m(t)$ and e(t) for a given gear pair depends primarily on the mean load T, and c_m is a function of the speed Ω, though a precise knowledge of c_m is difficult given the complicated dynamic friction conditions as summarized by He et al. (2007).

Some global relationships between L_p and sources or operating conditions may be suggested below. The L_p to e(t) relationship is 6 dB/octave, but note that e(t) itself depends on the load T, tooth profile including modifications and manufacturing errors. The L_p to speed (Ω) relationship is about 6 dB/octave or 40 dB/decade for a source that is mostly affected by the transmission error; this relationship works in a global sense up to the first geared system resonance. Similarly, the L_p to load (T) relationship is between 0 to 6 dB/octave since interactions among key sources dictate this effect. Thus one must exercise caution in employing such global relationships (Mitchell, 1971; Welbourne, 1979; Houser, 1992).

3. GEAR WHINE PERCEPTION

A. Frequency Domain Descriptors

Frequently, a single numerical index is assigned to rate product noise and its acceptance on some arbitrary, predetermined scale. However, the effectiveness of using such subjective ratings as an engineering tool for diagnostic purposes or to assess various engineering changes on the reduction of objectionable gear noise is limited because of several reasons. First, the resolution of a given subjective rating is limited by the auditor's ability to detect small changes in the character of the gear noise. Many times, gear noise is masked by noises from other sources both internal and external to the product. Second, many products must operate over a range of speeds (Ω) and loading (T) conditions. Dynamic gear mesh force, which is the primary exciter of gear noise, is known to be highly dependent on the mean transmitted torque and system gear pair dynamics. Further, system resonant behavior may significantly alter the amplitudes and frequency contents of the resulting gear noise. Product noise may be acceptable under certain operating conditions while unacceptable at others. In such cases, an overall rating index which accurately describes the acceptability of a particular product over its full range of operation is extremely difficult to obtain. Third, if a system containing multiple gear meshes is considered, the ability to distinguish subjectively between noise generated by individual gear meshes whose mesh frequencies (f_m) and/or harmonics coincide or nearly coincide at certain operating speeds may be impossible. Beating phenomenon, amplitude modulation, and frequency modulation effects may also exist which add further complexity to the gear noise. Finally, the repeatability of a subjective rating and correlation between individual auditors is always of concern. Personal inconsistencies among auditors and the inability to maintain uniform reference indices are responsible for sometimes large variations in subjective rating criteria, especially during those gear design and noise reduction programs which continue by necessity over relatively long periods of time.

We consider mostly the content and energy concentration in auto power spectra on a narrow band basis. Consider a discrete, one-sided, narrow band, auto power spectrum $W_{xx}(k\Delta f)$ of a gear signal x(t) with frequency resolution Δf which may represent sound pressure level, sound power level, gearbox acceleration, etc. Now consider a frequency bandwidth B_m centered about the m^{th} harmonic of gear mesh frequency f_m. We proceed on the premise that B_m is less than the closest critical bandwidth. Hence, the perceived sound energy within this band may be considered to be proportional to the weighted mean square value that is defined as:

$$\Psi_{wm}^2 = \sum_{k=k_1}^{k_2} w_m(k\Delta f) W_{xx}(k\Delta f). \qquad (2)$$

where w_m is the weighting function, and k_1 and k_2 are lower and upper band limits for the m^{th} mesh. Refer to Blankenship and Singh (1992a) for more details. Note that B_m may be chosen separately for each harmonic of f_m considered. Practical experience has shown that a uniform weighting works well for most cases. However, at other times, it is desirable to weight side-bands differently from mesh harmonics, especially when the bandwidth of significant modulation sidebands about a particular harmonic of gear mesh frequency exceeds the respective critical bandwidth or if modulation effects are clearly perceptible by human subjects. Next, we define an objective descriptor E_m which has been found to correlate with subjective gear whine ratings under certain circumstances. This weighted mesh energy estimator E_m represents the perceived acoustical or vibrational energy associated with the gear mesh and is formed from a linear combination of the Ψ_{wm}^2 computed about the m harmonic of f_m.

$$E_m = \sum_{i=1}^{m} \alpha_i \Psi_{wm}^2 \qquad (3)$$

where α_i is the weighting parameter (based on the locations of frequency bandwidth). The α_i is a scalar weighting parameter which is highly frequency dependent and may include such effects as human loudness perception as well as the transmission ratio between the band-limited energy of measured response signal x(t) and the band-limited energy level at the listener's ear. In order to obtain an even better objective, a gear whine descriptor E_s^* or L_{ms}^* is defined. It is based on multiple E_{ms} values from several transducer signals; here s represents the transducer index considered in the spatial average and α_s is the related weighting parameter.

$$E_{ms}^* = \Sigma_s \alpha_s E_{ms}; \quad L_{ms}^* = 10 \mathrm{Log}_{10} E_{ms}^* / E_{m,ref} \ . \qquad (4a, b)$$

B. Gear Whine Perception Example

The viability of the proposed rating scheme is demonstrated through a single mesh gear drive. A rating index based upon objective descriptors of measured data was developed which correlated with an existing noise quality rating scale. Eleven units were evaluated independently by three noise quality auditors, each of whom assigned a single numerical index to rate the acceptability of product noise on a predetermined scale from 1 to 10. A value of 1 (noisy) corresponds to intolerable annoyance while a value of 10 (quiet) is assigned to units which exhibit no perceptible gear whine. This subjective evaluation procedure may not be optimum since unavoidable biases are introduced by the predetermined scale, and further, no preference response testing methods were employed. However, variations of such subjective evaluation procedures pervade the field of machinery noise quality rating where more sophisticated methods are not practical or cost effective. Any objective descriptor or index must conform to the established noise quality rating methods employed by a particular product design or manufacturing group in order to be adopted by industry.

Measured vibration data were collected from three transducers: a single microphone located at a fixed distance and orientation from each unit (L_p); an accelerometer mounted on the gearbox housing directly over a shaft-bearing interface (L_{a1}); and an accelerometer mounted on a structural support which is attached directly to the gearbox housing (L_{a2}). The accelerometer locations were determined such that the localized dynamic response of the system was relatively insensitive to normal manufacturing errors and transducer mounting variations while being sufficiently close to the gear mesh source. Each unit was operated under identical speed and loading conditions corresponding to input shaft speed Ω = 1350 rpm, mesh frequency f_m = 450 Hz, and shaft frequencies f_{s1} = 22.5 Hz and f_{s2} = 9 Hz, respectively. This test condition was established by the auditors and corresponds to the operating condition where the potential for objectionable gear whine was greatest. The analysis frequency range is from 0 to 2000 Hz with Δf = 5 Hz. Hence $m \leq 4$ harmonics may be used in the construction of E_{ms}^* and L_{ms}^*. For this example, 3 transducer signals are used. A multivariate regression analysis was performed to determine the values of bandwidth and weighting parameters which gave the best straight line fit between L_{ms}^* and subjective rating in the least squares sense for m = 3. The resulting calibration curve $L_{ms}^* = 10 \mathrm{Log}_{10} E_{ms}^*$ (dB) versus average subjective rating is shown in Fig. 2 where the correlation coefficient $|\rho| = 0.983$. Here the reference value of $E_{ms}^* \left(L_{ms}^* = 0 \, \mathrm{dB} \right)$ corresponds to a subjective ranking of 6. The above example further suggests that the correlation between L_{ms}^* and subjective rating must be viewed within a confidence interval of subjective rating ± 1 with respect to the 1 to 10 subjective rating scale employed in this study. This is consistent with the

observed resolution and repeatability (estimated ± 1) of the subjective auditor ratings. Refer to Blankenship and Singh (1992a) for more details.

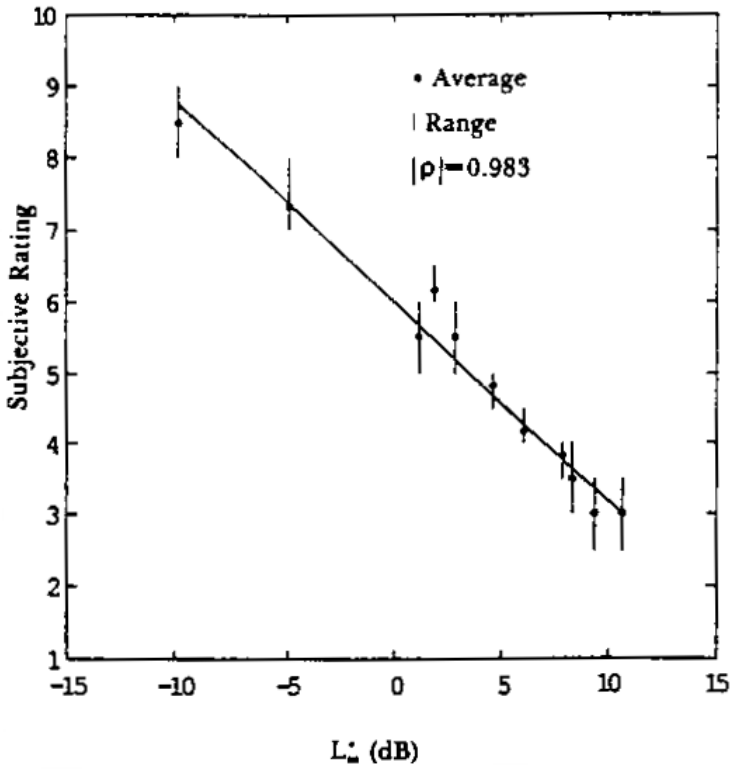

Figure 2: Subjective ranking versus perceived gear whine level $L^*_{ms} = 10\,Log_{10}E^*_{ms}$ (in dB) obtained from spatially averaged microphone (L_p) and accelerometer signals (L_{a1} and L_{a2}) with m = 3, bandwidth (B_m) ranging from 10 to 70 Hz and correlation coefficient $|\rho|$= 0.983.

4. WHINE NOISE PREDICTION MODELS

A. Literature Review

The literature on the vibro-acoustic models of the entire geared system is rather sparse. The vibration transmission path through bearings has been well described by the stiffness matrix that was analytically formulated by Lim and Singh (1989, 1990a,b, 1991a,b). Rook and Singh (1996, 1998) analyzed the gearbox using the mobility synthesis method and derived a procedure of calculating narrow-band vibratory power flows. They also recognize rolling element bearings as a multi-dimensional compliant and dissipative connection. Moreover, the vibration behavior of the gearbox housings has been examined by using finite element analysis (FEA), experimental modal analysis and statistical energy analysis (SEA) methods. For instance, Lim and Singh (1990a,b) developed a finite element model of flexible casing to predict bearing and mount transmissibilities in a simple geared system. Lim and Singh (1991a,b) developed a two sub-system SEA model which included an analytical description of the coupling loss factor associated with the vibration transmission through rolling element bearings.

To predict sound radiation from the gearbox, prior researchers have relied on either simple radiation efficiency models or large scale numerical codes (such as the boundary elements). However, a combination of finite and boundary element models often requires extensive computational time while yielding minimal insight. Jacobson et al. (1996) predicted the radiation

efficiency of a gearbox plate using ideal radiators like monopole, dipole, cylinder, and the like but achieved limited success when compared with in-situ radiation measurements. Such simplified models yield only global trends and do not adequately describe the modal radiation characteristics of a gearbox. Kartik and Houser (2003) proposed a semi-empirical frequency-response based model to predict noise radiation from gearbox housings with a multi-mesh gear set. Also, they utilized the broad-band radiation efficiency model of a rectangular plate; again their model yields only a broad trend over a range of gear mesh frequencies. Recently, Singh et al. (2007) developed a semi-empirical model for predictions of the radiated whine noise by combining a linear time-invariant model of the internal geared system with measured vibro-acoustic transfer functions of the structural paths (from gear/pinion motions in two directions to the radiated sound). Yet, the same system is then analyzed using analytical path and radiator models by He et al. (2008b). Both approaches are described in subsequent sub-sections.

B. Source-Path-Receiver Model for Gear Whine

The source-path-receiver concept of Fig. 3 is employed to predict gear whine noise excited by both the static transmission error (STE) and sliding friction. These two excitations are inputs to a linear 8 degree-of-freedom (DOF) model, which is characterized by natural frequencies (ω_r) and mode shapes (ϕ_r). This study focuses on the prediction of dynamic bearing forces in both the line-of-action (LOA) and off-line-of-action (OLOA) directions. These forces are coupled at the bearings with housing structures which cause the out-of-plane vibrations of housing panels. The structural velocity of the housing is radiated as sound pressure, where it is perceived by the receiver. A simple model utilizing measured acoustic-structural transfer functions (pressure/acceleration or p/a) is then employed to predict the sound pressure level (SPL) at the gear mesh harmonics. The transfer functions are measured on the NASA GRC noise rig for a unity-ratio spur gear pair system. An order of magnitude comparison could thus be made to experimental data at selected mesh harmonics. Note that the same gear set and rig were used to generate the transfer functions and to collect the sound and vibration data. This should allow us to assess the relative importance of two gear noise sources of Fig. 3.

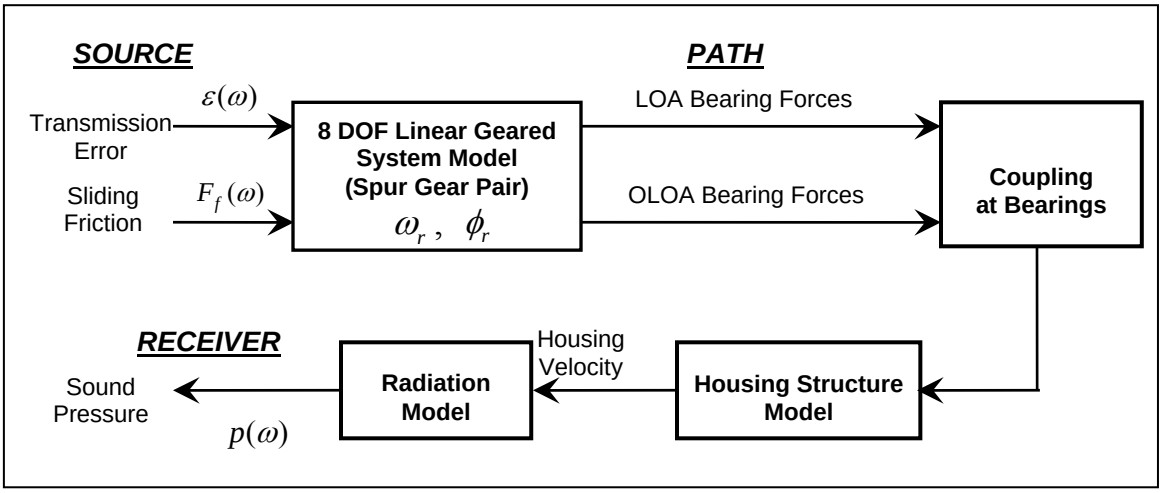

Figure 3: Conceptual description of the vibro-acoustics of a geared system with two excitations, given linear system assumption

The schematic for the 8 DOF gear pair system is shown in Fig. 4. The pinion (subscript p) and gear (subscript g) each has one vibratory angular motion θ as well as two translational motions x and y corresponding to the LOA and OLOA motions. The base radius and inertia are denoted by R and J with averaged mesh stiffness represented by k_m. Symbol m represents the mass of the pinion/gear along with contributions from the respective shafts. The inertias of the motor and load are denoted by J_d and J_L, and the torsional input and output shaft stiffness (viscous damping coefficients) are given as k_{Td} and k_{TL} (c_{Td} and c_{TL}). The input and output torques at the motor and load are T_d and T_L. Here, both shafts are modeled as simply supported beams with the effective shaft-bearing stiffness elements designated by k_x and k_y in the LOA (x) and OLOA (y) directions, respectively. The corresponding viscous damping coefficients of similar notation are also included. Besides the loaded STE displacement excitation ε(t) at the gear mesh in the LOA direction, the friction force excitation $F_f(t)$ is assumed to act externally at gear mesh in the OLOA direction.

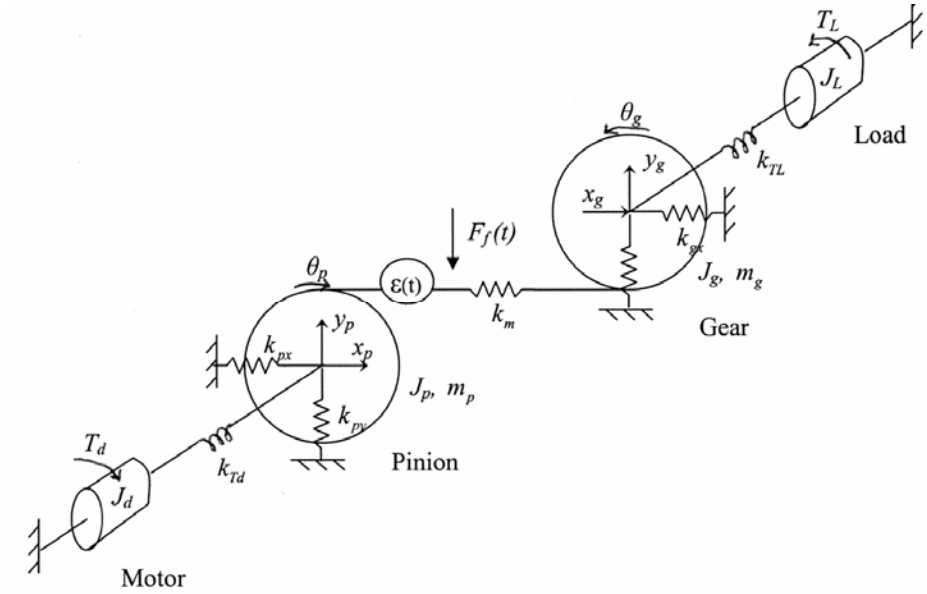

Figure 4: Schematic of the whine source (8 DOF geared system) model with two gear noise sources for a spur gear pair (damping elements not shown)

C. Gear Whine Prediction using Empirical Path and Receiver Models

Using the concepts of Figs. 3 and 4, predictions of dynamic bearing forces provide structure-borne excitations to the gearbox housing, which could significantly amplify the transmitted vibrations and noise since the panels are efficient radiators. By relating the dynamic bearing forces to measured sound pressure levels (L_p), predictions can be directly compared with experimental data. The LOA and OLOA accelerations at the mesh harmonic frequencies are combinations of the accelerations due to translational and rotational motions; they could be derived as follows, where $f = mf_m$: $a_x(f) = \ddot{x}_g + R_g\ddot{\theta}_g$ and $a_y(f) = \ddot{y}_g$. These dynamic responses, along with the transfer functions measured in both the LOA and OLOA directions, could provide the sound pressure at the gear mesh frequencies: $p_x(f) = H_x a_x(f)$ and $p_y(f) = H_y a_y(f)$. Here, H_x and H_y (in the units of μPa/(in/s^2)) are the acoustic-structural (p/a) transfer functions measured in the LOA and OLOA directions, in which a is the translational gear acceleration (in/s^2). Although the phase of the sound pressures in the two directions is unknown,

a maximum and minimum could be determined by assuming an in-phase and out-of-phase relationship, respectively. Thus, a range of possible values could be predicted, such that $p_{min} \leq p(f) \leq p_{max}$, where $p_{max} = p_x + p_y$, $p_{min} = p_x - p_y$. However, prediction results are only given in terms of the maximum values due to the space limitation. The sound pressure is converted into unweighted L_p (dB re 20 μPa). The LOA and OLOA gear accelerations are calculated at the mesh harmonics assuming realistic forces predicted by the gear contact mechanics software. The sound pressures are determined for the range of mean loads (T) from 500 to 900 in-lb.

As conceptually shown by the block diagram in Fig. 3, this measured transfer function is essentially a combination of several gear dynamic, housing structural, and radiation transfer functions within the system.

$$\frac{p}{a_g} = \left(\frac{p}{a_h}\right)\left(\frac{a_h}{F_{br\_ext}}\right)\left(\frac{F_{br\_ext}}{F_{br\_int}}\right)\left(\frac{F_{br\_int}}{a_g}\right). \tag{5}$$

Here, F_{br_int}/a_g is the bearing force/gear acceleration transfer function and F_{br_ext}/F_{br_int} represents the coupling at the bearings which relates the internal forces to the external forces. The latter transfer function (force transmissibility across the bearings in a multi-dimensional manner) could not be directly measured. The external forces excite the gearbox housing structural acceleration through a_h/F_{br_ext} and then radiated as sound pressure from the radiating surfaces, defined by the p/a_h transfer function. Refer to Singh et al. (2007) for more information.

D. Comparison with Noise Measurements

The Gear Noise Rig at NASA Glenn was operated with the unity ratio spur gear set. Vibro-acoustic responses were measured at various microphone locations within the NASA gearbox. In the experiment, the mean torque was varied over a range from 500 to 900 in-lb. at a speed of 4875 Hz. The oil temperature was also varied in these experiments, and the case of 140 °F (60°C) (measured for the oil flinging-off the gears as they enter into mesh) is utilized for comparison. Both LOA and OLOA bearing forces are predicted for the example case (unity-ratio NASA spur gear pair with tip relief) with parameters of the pinion/gear given as follows: number of teeth = 28; outside diameter = 3.738 in; root diameter = 3.139 in; diametral pitch = 8 in^{-1}; center distance = 3.5 in; pressure angle = 20°; face width = 0.25 in; tooth thickness = 0.191 in; and elastic modulus = 30×10^6 psi. Predictions are then converted from time domain into frequency domain by using the fast Fourier transform (FFT) analysis method. The predicted results were normalized with respect to the maximum sound pressure (μPa) occurring at the 2nd mesh harmonic and a mean load of 900 in-lb. Figure 5 shows the normalized amplitudes for the first four mesh harmonics across the range of loads. The comparison presented here is only on an order of magnitude basis. Note the measured transfer functions may contain errors; further, we may not have accurately modeled all of the parameters. Sound level of 1st harmonic is expected to increase as the load increases since tip relief is applied with a "optimal" load of 600 in-lb; however, the measured data shows the opposite, which has a relative minimum at 800 in-lb. while the maximum amplitude corresponds to a load of 500 in-lb. It is possible that the airborne source is affecting the measurement at this mesh harmonic, while the experimental study focused only on measuring the structure-borne noise paths. The spectra of the 2nd mesh harmonic show similar behavior with increases in load. Both the prediction and measurement have maximum L_p at the 2nd mesh harmonic. In fact, the rest of the harmonics all generally show an increasing trend versus load. The predicted L_p harmonics seem to increase somewhat linearly with torque. Also, prediction shows a significant amplitude for the 3rd harmonic, which is greater than the 1st harmonic. However, L_p measurements show the 1st harmonic is more significant.

Definitive conclusions could not be drawn based on the limited results and a lack of accurate system parameters. Nevertheless, the implementation of the proposed noise prediction model highlights a key area for improvement over the existing literature, and thus it should be pursued in future research.

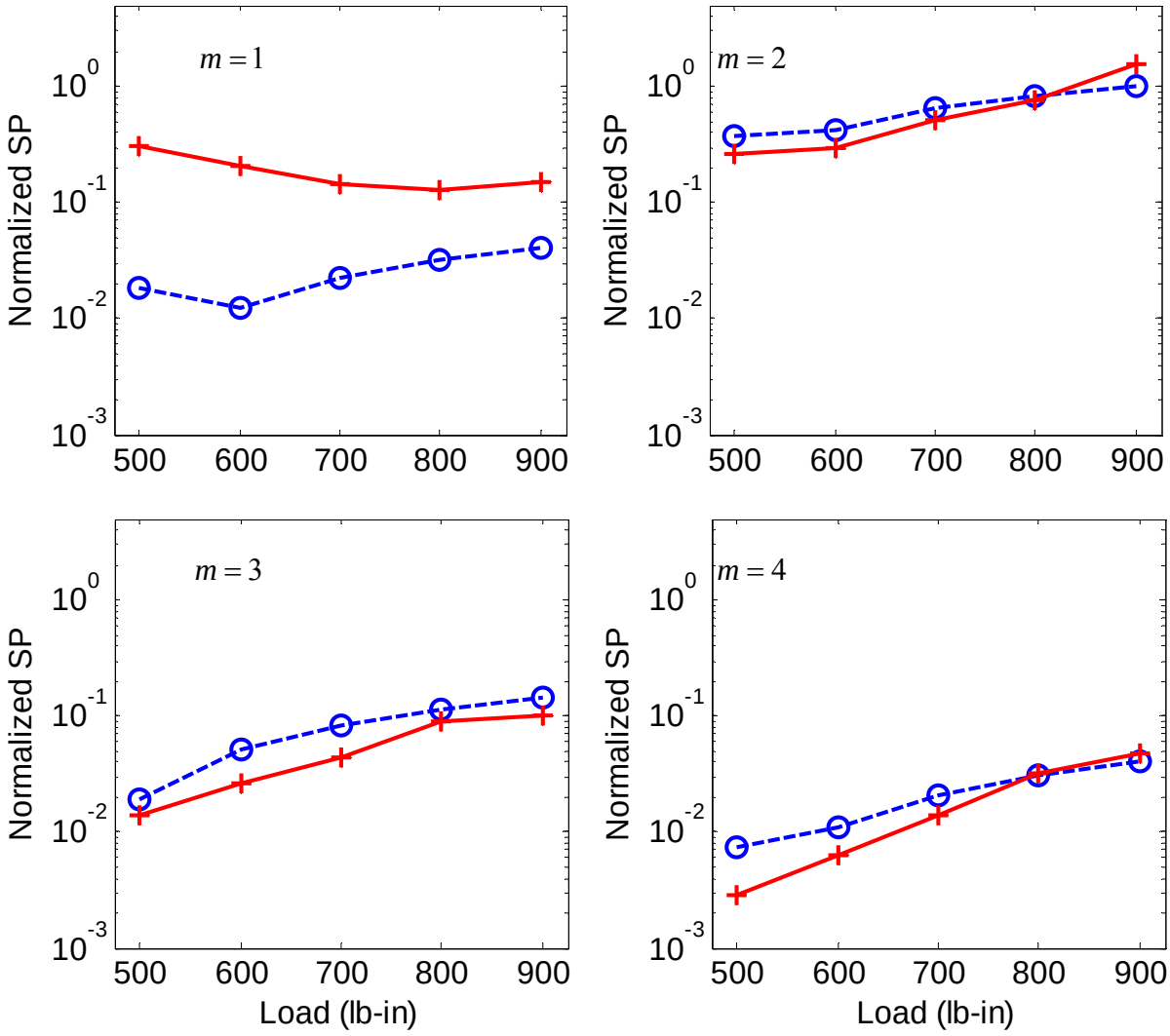

Figure 5: Comparison of the normalized sound pressure (SP) predictions with measurements at the first four gear mesh harmonics (m = 1, 2, 3, 4). Key: —+—, measurements; –⊖–predictions. Note that this formulation utilizes empirical structural path and receiver models.

E. Gear whine Prediction using Analytical Path and Receiver Models

Most gear noise researchers have assumed that the static transmission error (STE) is the main source of whine (steady state noise at gear mesh frequencies and side-bands). Consequently, transmission errors are minimized in a methodical manner via tooth modifications. However, high precision gears are still noisy in many applications. One plausible explanation is that the sliding friction becomes a potential noise source, especially in spur gears at certain torques or tribological conditions. Accordingly, we consider two concurrent excitations, namely the unloaded static transmission error and sliding friction, to a geared system. Dynamic forces at the bearings are illustrated in Figure 6 over a range of operating torques (T_p). Objectives of this

analytical formulation are: (1) Develop a refined source-path-receiver model that characterizes the structural paths in two directions and propose analytical and efficient computational tools to predict noise radiated from the gearbox panels; and (2) quantify the relative contributions of transmission error versus sliding friction noise to the overall whine noise, and validate predictions of the structural transfer functions and sound pressure with measurements for one example case (NASA gearbox with spur gears) as shown in Figure 7.

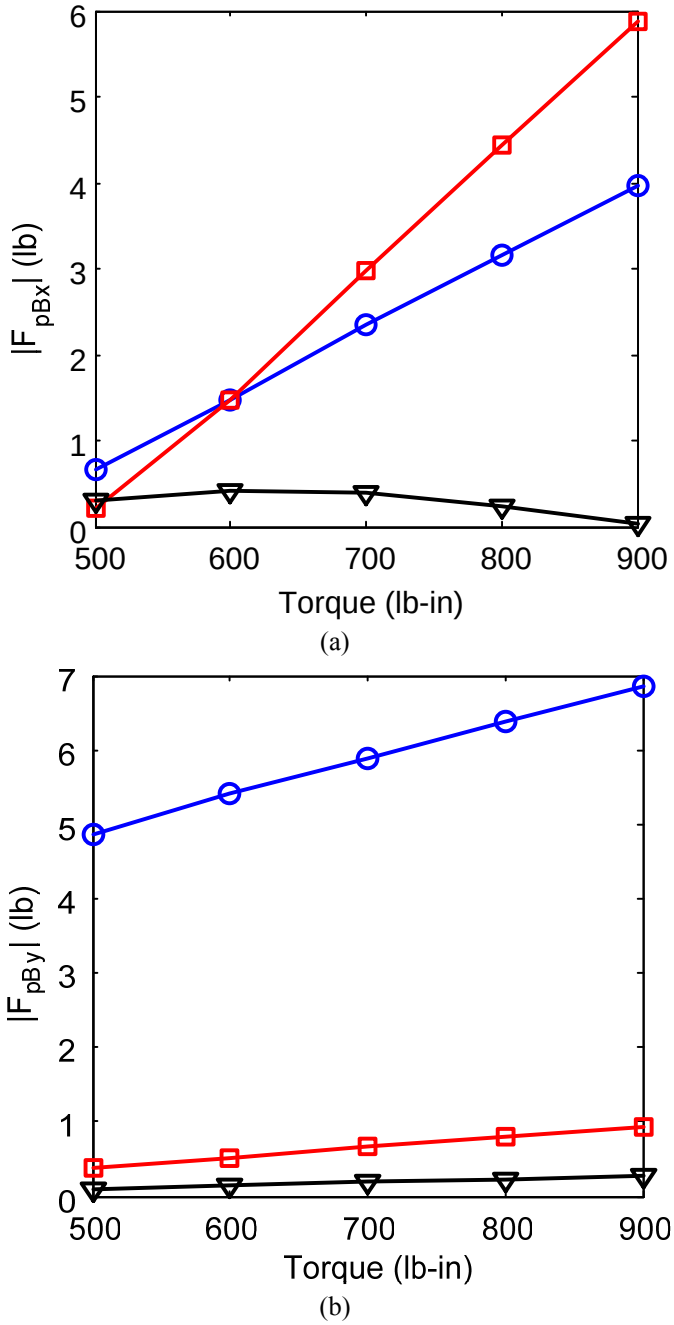

Figure 6: Dynamic bearing forces predicted over a range of T_p given Ω_p = 4875 RPM and 140 °F. (a): Line-of-action (LOA) bearing force in the x direction; (b) off-line-of-action (OLOA) bearing force in the y direction. Key: m is the gear mesh frequency harmonic. Key: —○—, m = 1; —□—, m = 2; —▽—, m = 3.

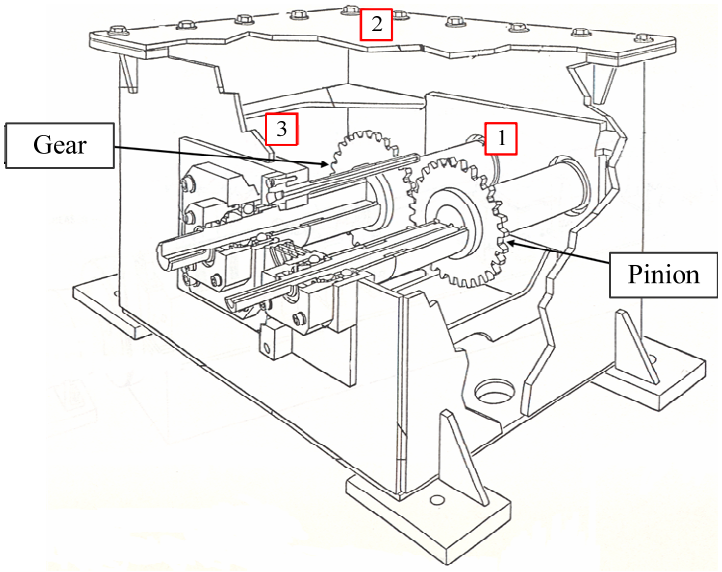

Figure 7: Schematic of the NASA spur gearbox.

Force excitations are coupled at each bearing via a stiffness matrix $[K]_{Bm}$ (of dimension 6) that is calculated by using the algorithm proposed by Lim and Singh (1990a). Nominal shaft loads and bearing preloads are assumed to ensure a time-invariant $[K]_{Bm}$. In order to focus on the transmission error and sliding friction paths in the LOA and OLOA directions respectively, $[K]_{Bm}$ is intentionally reduced into a 2 by 2 matrix by neglecting the moment transfer terms and assuming that no axial force is generated by the spur gear sub-system. The transfer function of the combined source-path sub-systems is predicted as follows where ω (rad/s) = 2πf (Hz):

$$\tilde{H}_{S-P} = \tilde{H}_p(\omega)\cdot\tilde{H}_p(\omega) = \tilde{H}_s(\omega)\cdot\frac{\tilde{Y}_{plate}(\omega)}{\tilde{Y}_{bearing}(\omega)}; \tag{6}$$

$$\tilde{Y}_{plate}(\omega) = \frac{\tilde{V}_{plate}(\omega)}{\tilde{F}_{bearing}(\omega)}; \qquad \tilde{Y}_{bearing}(\omega) = \frac{\tilde{V}_{bearing}(\omega)}{\tilde{F}_{bearing}(\omega)}; \tag{7a,b}$$

where $\tilde{Y}_{plate}(\omega)$ and $\tilde{Y}_{bearing}(\omega)$ are the transfer and driving point mobilities for the (top) plate and the bearing; these are derived from the finite element model of the gearbox by using the modal expansion method with 1% structural damping for all modes. Further, $\tilde{H}_s(\omega)$ is the motion transmissibility from gear mesh to translational bearing responses (in LOA or OLOA directions) by using the 8DOF linear time-invariant spur gear model. Note that such a lumped model is inadequate to capture the bending and flexural modes of the gear blanks and shafts.

Figure 8(b) shows that the measured motion transmissibility (OLOA direction) from gear mesh to the bearing compares well with predicted $|\tilde{H}_S(\omega)|$ based on the linear time-invariant model. In Figure 8(c), the predicted motion transmissibility $|\tilde{H}_{S-P}(\omega)|$ from gear mesh to the top plate correlates reasonably well with measurement (Fig. 8(a)) given complexity of the system. First, assume that (i) the bearing forces predicted by the source model are in phase at either bearing end for the pinion (or gear) shaft; and (ii) the bearing forces of pinion and gear are same

in magnitude but opposite in directions due to the symmetry of unity ratio gear pair. Second, the overall structural paths are derived for the transmission error controlled LOA (or x) path and the friction dominated OLOA (or y) path in terms of the combined (effective) transfer mobilities $\tilde{Y}_{e,x}(\omega)$ and $\tilde{Y}_{e,y}(\omega)$:

$$\tilde{Y}_{e,x}(\omega) = \sum_{n} \tilde{W}_{p,x,n} \tilde{Y}_{p,x,n}(\omega) - \sum_{n} \tilde{W}_{g,x,n} \tilde{Y}_{g,x,n} \tag{8}$$

$$\tilde{Y}_{e,y}(\omega) = \sum_{n} \tilde{W}_{p,y,n} \tilde{Y}_{p,y,n}(\omega) - \sum_{n} \tilde{W}_{g,y,n} \tilde{Y}_{g,y,n}(\omega) \tag{9}$$

where $\tilde{W}$ is the empirical weighting function (10 dB applied over the spectrum), and the subscript n is the index of the two ends of pinion/gear shafts. The proposed method thus provides an efficient tool to quantify and evaluate the relative contribution of structural path due to sliding friction. The top plate velocity distribution $\tilde{V}_{top}(\omega)$could then be predicted, as shown below, where $\tilde{F}_{p,B,x}(\omega)$ and $\tilde{F}_{p,B,y}(\omega)$ are the pinion bearing forces predicted by the source model in the LOA and OLOA directions.

$$\tilde{V}_{top}(\omega) = \frac{1}{2}\tilde{F}_{p,B,x}(\omega)\tilde{Y}_{e,x}(\omega) + \frac{1}{2}\tilde{F}_{p,B,y}(\omega)\tilde{Y}_{e,y}(\omega) \tag{10}$$

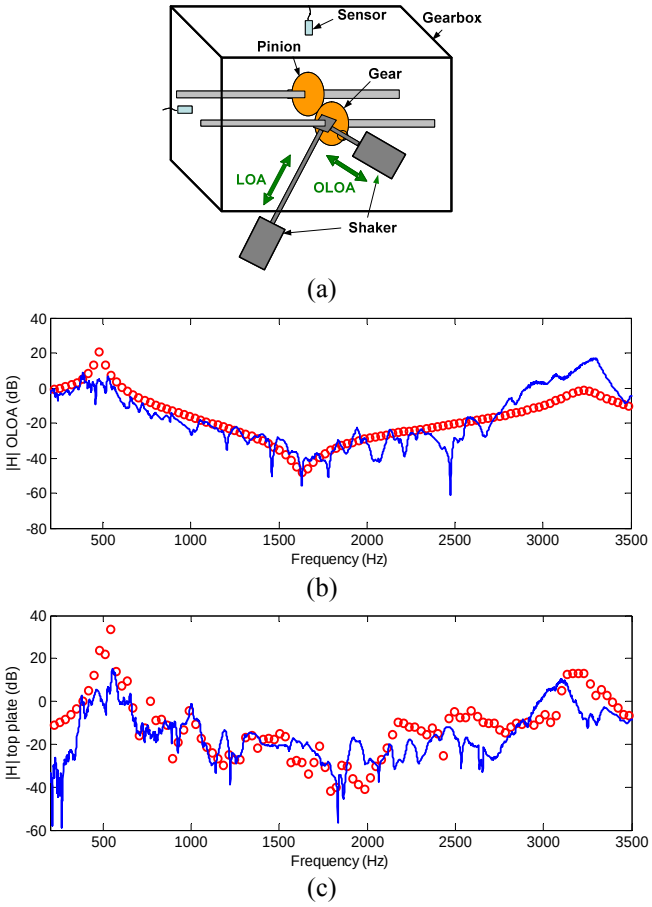

Figure 8: (a) Experiment used to measure the structural transfer functions; (b) Comparison of the transfer function magnitudes from gear mesh to bearings; (c) Comparison of the transfer function magnitudes from gear mesh to a sensor on the top plate (gearbox). Key: ○, measurements; —— predictions.

F. Prediction of Radiated Noise

Since the rectangular top plate of the gearbox is the main radiator due to its relatively high mobility, Rayleigh integral is used to approximate the sound pressure by assuming that the top plate is placed in an infinite rigid baffle and each elementary plate surface is an equivalent point source in a rigid wall. The sound pressure amplitude at frequency ω (rad/s) is given as follows where ρ is the air density, $\widetilde{Q}_i(\omega) = \widetilde{V}(\omega)\Delta S_i$ is the source strength of i^{th} equivalent point source with area ΔS_i, $k(\omega)$ is the wave number, and r_i is the distance from the i^{th} source to the receiver:

$$\widetilde{P}(\omega) = \frac{j\omega\rho}{2\pi}\sum_i \frac{\widetilde{Q}_i(\omega)}{r_i} e^{-jk(\omega)r_i} \tag{11}$$

For the calculation of whine noise, ω is chosen to coincide with first three gear mesh frequencies of interest; ΔS_i is chosen such that its dimension (on the top plate) is smaller than ¼ of the wave-length at the highest gear mesh frequency. The overall noise is then calculated by combining the contributions of all equivalent sources at the receiver. Compared with conventional boundary element analysis, Rayleigh integral approximates sound pressure in a fraction of the computation time. Hence, it is more suitable for parametric design studies. However, the Rayleigh integral may give large errors for sound pressure prediction if applied to strongly directional, three dimensional fields. Such errors are not significant in our application due to a flat top plate and favorable surroundings (such as rigid side plates and the anechoic chamber).

As an alternative to the Rayleigh integral technique, a newly developed algorithm based on the substitute source approach (Pavic, 2005, 2006) is used to compute the radiated or diffracted sound field. It is conducted by removing the gearbox and introducing acoustic sources within the liberated space which yield the desired boundary conditions at the box surface (Neumann problem). Solutions are obtained in terms of the locations and/or the strengths of the substitute sources by minimizing the error function between original and estimated particle velocity normal to the interface surface (Pavic, 2006).

G. Comparison with Noise Measurements

Figure 9 compares the sound pressure measured at the microphone 6 inches above the top plate to predictions by using both the Rayleigh integral as well as the substitute source methods over a range of pinion torque given Ω_p = 4875 RPM and 140 °F. Notice that the second mesh harmonic, which is most susceptible to the sliding friction, becomes increasingly more dominant at higher torques for our example case. Proposed Rayleigh integral method and substitute source technique are capable of calculating the acoustic field and quantifying the frictional noise. Next, Figure 9 compares the sound pressure level predicted under T_p = 500 lb-in (close to the "optimal" load where transmission error is minimized) and under high torque with T_p = 800 lb-in. At each gear mesh frequency, individual contributions of transmission error (via the LOA path) and frictional effects (via the OLOA path) are compared to the overall whine noise. Observe in Figure 10(a) that near the "optimal" load, sliding friction induced noise is comparable to the transmission error induced noise (especially for the first two mesh harmonics); thus sliding friction should be considered as a significant contributor to the whine noise. However, at "non-optimal" torques in Figure 10(b), friction induced noise is overwhelmed by the transmission error noise, thus sliding friction could be negligible under such conditions. This confirms that the sliding friction should be viewed as a potential contributor to structure-borne noise for high precision, high power density geared systems.

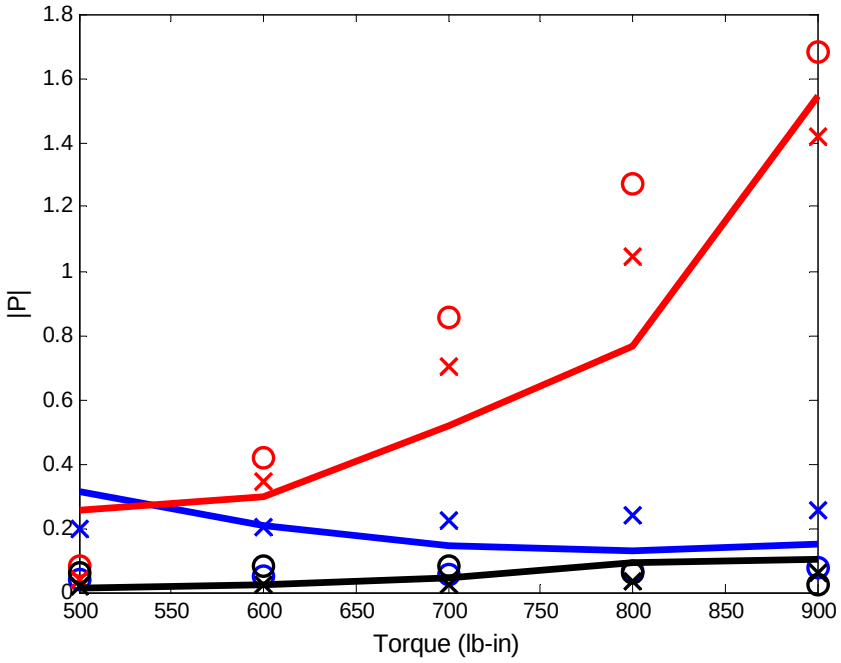

Figure 9: Sound pressures (Pa) at the first three gear mesh frequencies (with speed Ω_p = 4875 RPM) over a range of torque T_p at 140 °F. Key: ——, measurements (6" above the top plate); O, Rayleigh integral predictions; ×, substitute source predictions. Color code: Blue, gear mesh frequency harmonic m = 1; red, m = 2; black, m = 3. Note that this formulation utilizes analytical descriptions of sources, paths, and radiators.

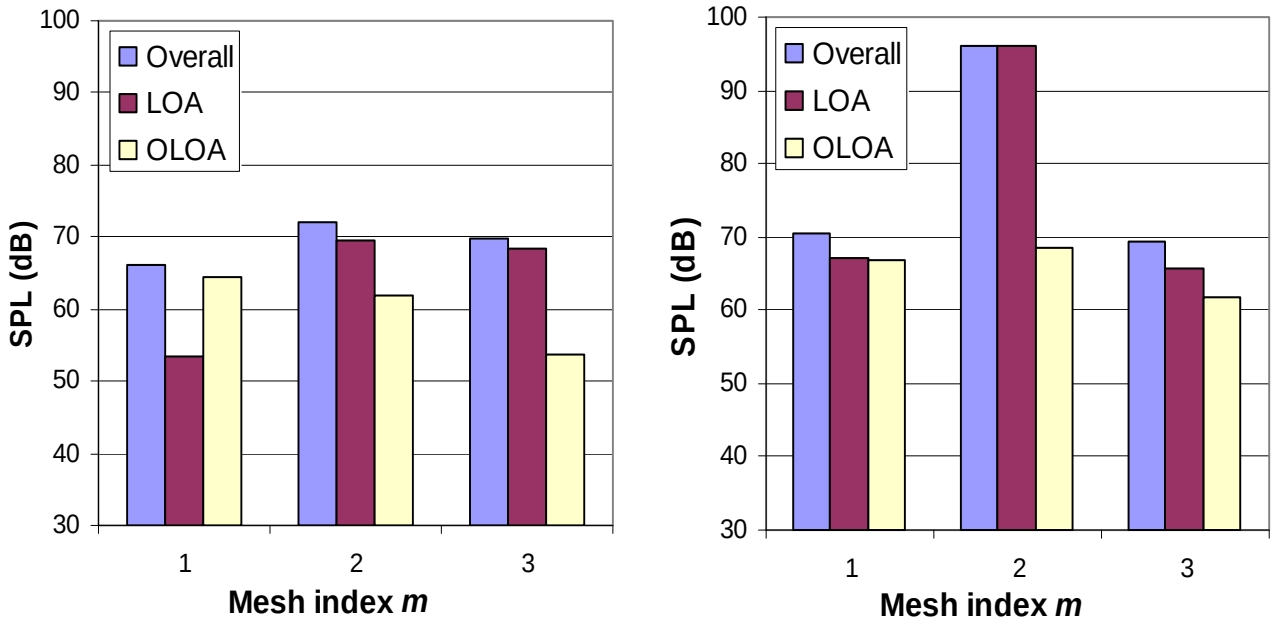

Figure 10: Overall sound pressure levels (dB re 2e-5 Pa) and their contributions predicted at 6" above the top plate under Ω_p = 4875 RPM and 140 °F. (a) Mean load T_p = 500 lb-in (optimal load for minimum transmission error); (b) mean load T_p = 800 lb-in. Key: LOA = line-of-action; OLOA = off-line-of-action.

5. WHINE NOISE CONTROL STRATEGIES

The first step in the noise control strategy is the diagnostic of the problem. This implies detailed noise and vibration experiments over a range of applicable torques and speeds including frequency spectra, waterfall plots, and order tracks. As suggested in sections 2, 3, and 4, gear mesh frequencies, ghost frequencies (if any), resonances, and other peaks must be properly identified given the geared system kinematics, vibration modes, and forced responses under the real operating conditions. Correlation between static (or dynamic) transmission error measurements, casing accelerations, and sound pressure levels are desirable. For the whine problem, gear profile and lead measurements must be made to assess profile errors due to manufacturing processes along with a determination of the contact patterns under a specific torque T (for instance). Next, the gear contact mechanics codes (such as Ohio State's Load Distribution Program (LDP), 2009) may be utilized to calculate e(t) and $k_m(t)$ as well as their spectral contents at mf_m. At this stage, the effects of gear design parameters including profile modifications may be studied. The intent is to minimize the excitations at a given T. Refer to Houser and Singh (2008) for some examples. Also, examine the natural frequencies and torsional-flexural modes of the internal (rotating) system. Based on the frequency and forced responses of the linear system (with no tooth separation), an assessment of the dynamic forces at the gear mesh interfaces and bearings can be made. These excitation forces can then be related to the radiated sound pressures via analytical or computational models for transmissibility across the bearings, casing, and supporting structure motions and radiation mechanisms. These steps are illustrated in section 4.

Overall, the whine noise should be viewed as the geared system noise problem though the vibrational sources originate at the gear interface(s). In the case of an open geared system, direct radiation from the gear meshes may occur. Thus, one must examine strategies to reduce noise by focusing at one or more of the following: gear design and kinematics, profile and lead modification, surface finish and lubrication considerations, torsional-flexural modes of the internal system, modes of the gear blanks, stiffness of shafts and bearings, stiffness matrix of the rolling element bearings, misalignments and eccentricities casing dynamics, casing mounts and supporting structures, and finally the radiation properties of the casing and other surfaces. This is clearly illustrated in section 4. Damping treatments either on the gear blanks or the casing structure would work only when resonances are involved. Given strong dynamic interactions between source(s) and structure-borne noise paths, caution must be exercised to ensure that overly compliant paths or mounts do not alter the sources at the meshes. Multi-disciplinary skills are often needed to solve difficult gear whine problems.

Several researchers including Houser (1992, 2007), Houser and Singh (2008), Mitchell (1971), and Welbourne (1979) list typical reductions in noise levels due to many design and operational factors. A summary of key factors is given below though the user must exercise cautions. 1. Lower mesh frequencies f_m (by decreasing the number of teeth or the speed) to reduce L_p at lower frequencies (say below 1 kHz). 2. In the absence of strong resonances, L_p is proportional to 20 Log_{10} |e| where |e| is the magnitude of static transmission error. 3. Tip relief and other profile modifications reduce sound, generally at the design loads. 4. Helical gears are generally quieter over spur gears. 5. Gears with high contact ratios reduce the excitation. 6. Mobility mismatches in internal and external systems yield some benefits provided the source level does not change. 7. Bearing type and its installation could affect the noise levels by up to

6 dB. Similarly, many other assertions may be made though many of the reported claims are rather application specific and depend on the gear accuracies and operational conditions.

6. ANATOMY OF GEAR RATTLE SOURCES

The sources of rattle or periodic vibro-impacts in mechanical systems are clearance non-linearities, which include backlashes, multi-valued springs, hysteresis, and the like. Table 2 lists some key parameters that influence conditions for single sided or double sided impacts in a vehicle transmission. We should recognize the following: (i) the rattle problem is generally a dynamic system problem, i.e., it is not a gear dynamic issue (such as whine); (ii) a suitable nonlinear torsional model of the system is needed to understand the basic characteristics, to find optimal design solutions, and to examine signal processing and sound perception issues; and (iii) rattle problems are best analyzed in time domain even though we can use other domains to obtain some fundamental properties of a vibro-impact oscillator. Given the space limitations, only an overview is presented. For details, refer to Singh et al. (1989, 2007) and other literature cited in these articles.

In practical rattle problems, many different elements and clearances are encountered (e.g., gears, bearings, splines, and clutches). Consequently the dimension can be quite large, which is inefficient from a computer simulation point of view. Therefore, in the formulation, reduced order torsional models must be utilized; however, the appropriateness of such models is difficult to assess a priori. Furthermore, the non-analytic nature of vibro-impact problems presents particular difficulties at the simulation stage, including ill-conditioning and numerical "stiffness." A variety of numerical algorithms, including direct time integration and harmonic balance techniques, have been investigated for these types of problems. Refer to Singh (2007) for details. Also not to be overlooked are the problems encountered in the classification of rattle sound quality or perception.

Table 2: Factors influencing rattle levels in vehicle transmissions (manual type)

- Engine type and torque pulsations (gasoline, diesel, turbo-charged)
- Mean torque or preload
- Flywheel and inertial distribution within system
- Clutch dampers [spring rates, friction, hysteresis], damper, etc.
- Backlash or clearances (gears, synchronizers, hub splines, bearing)
- Drag torque, oil level and oil viscosity, temperature, etc.
- Impact damping mechanism
- System load affecting torsional dynamics
- System resonances
- Structure-borne or airborne path(s)
- Other factors unique to the application

7. RATTLE MODELS

A. Example: Vehicle Transmission Rattle

Figure 11 shows a generic physical model of an automotive manual transmission. The sign convention for the torsional displacements $\theta_i(t) = \theta_{mi}(t) + \theta_{pi}(t)$, i = 1-4, is shown in Figure 11, where $\theta_{mi}(t)$ and $\theta_{pi}(t)$ are mean and vibratory parts, respectively. The input gear moment of inertia I_3 also includes the reflected moments of inertia from other gears: i.e., the moments of inertia of all of the input gears and those of the intermediate gears, other than the one used for I_4 calculation, are lumped into one term to yield I_3. Non-linear characteristics of a simplified clutch damper torque T_c are shown in Figure 12. The elastic compression force F_b between the

conjugate gear pair of radii R_3 and R_4 is given in Figure 13. Here, the gear meshing stiffness k_g and backlash ($2x_b$) are assumed to be constants.

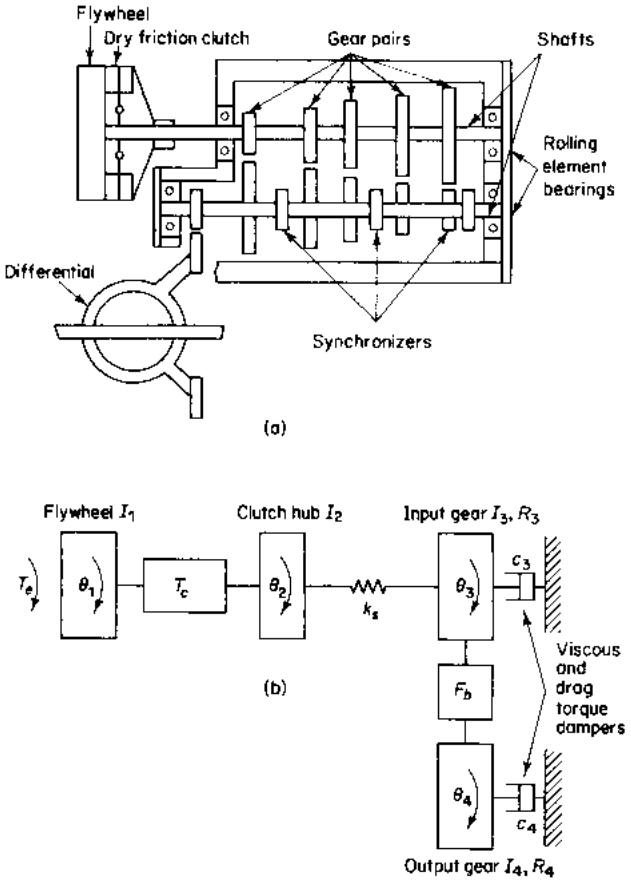

Figure 11: Physical model for the neutral gear rattle problem. (a) Automotive manual transmission schematic; (b) a simplified torsional model.

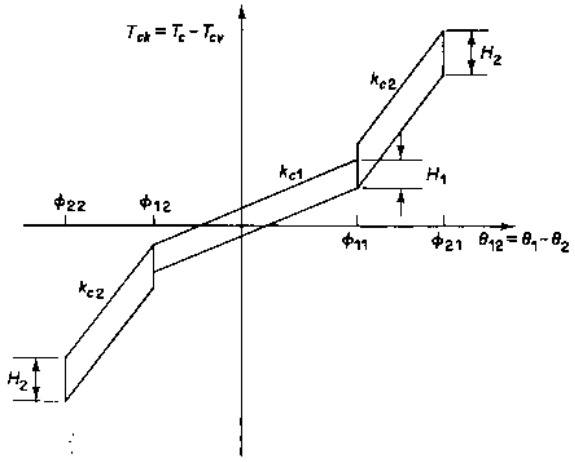

Figure 12: Dynamic characteristics of a simplified clutch damper. Here $T_{cv} = c_{12}\dot{\theta}_{12}$ is the viscous damping torque, k is the stiffness, and H is the hysteresis. This curve is asymmetrical in operational angles (ϕ); i.e. $\phi_{11} \neq \phi_{12}$ and $\phi_{21} \neq \phi_{22}$. See Singh et al. (1989) for details.

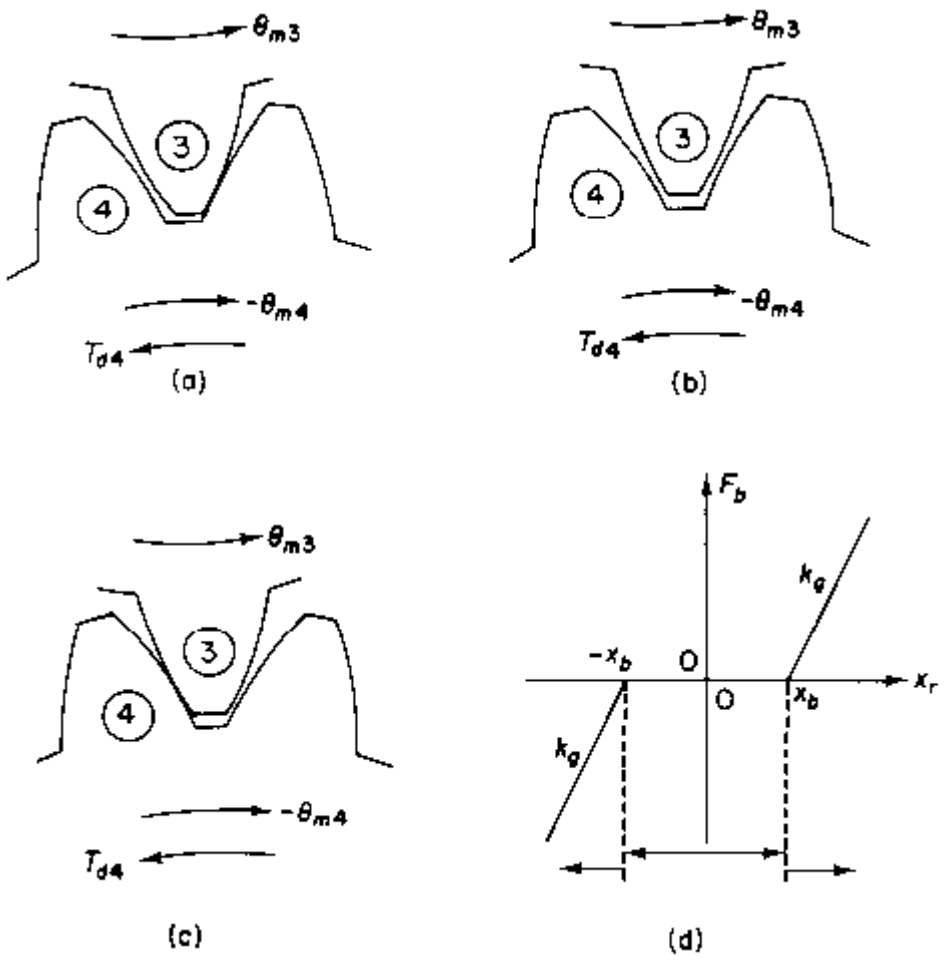

Figure 13: Meshing gears and gear mesh force F_b. (a) Gears in contact on the driving side; (b) gears separated; (e) gears in contact on the driven side; (d) elastic compression force (F_b) with gear teeth meshing stiffness (k_g) and backlash ($2x_b$). Here, the relative displacement is $x_r(t) = R_3\theta_3 + R_4\theta_4$.

B. Gear Rattle Criteria

Vibro-impacts or rattle should not occur when the gears remain in contact at the driving side, as shown in Figure 13(a); this implies that $x_r(t) \geq x_b$. Rattle between conjugate gears will obviously take place under the following conditions: (i) gears are separated and free to move within the backlash as shown in Figure 13(b), and (ii) the gears are in contact on the driven side as shown in Figure 13(c) - since this case is not compatible with the mean torque requirements, separation will occur very quickly; consequently, Figure 13(c) is an unstable case and must be avoided. Mathematically, a rattle criterion can be given in terms of $x_r(t)$ as

$$x_r(t)\begin{Bmatrix} < x_b : \text{rattle} \\ \geq x_b : \text{no rattle} \end{Bmatrix} \tag{12}$$

By using a mathematical model and noting that $T_{d4} - I_4\ddot{\theta}_4 > 0$ is equivalent to $x_r(t) - x_b > 0$, but $T_{d4} - I_4\ddot{\theta}_4 = 0$ is not equivalent to $x_r(t) - x_b = 0$, the rattle criterion can be reformulated as

$$T_{d4} - I_4\ddot{\theta}_4(t)\begin{Bmatrix} \leq 0 : \text{rattle} \\ > 0 : \text{no rattle} \end{Bmatrix} \tag{13}$$

This implies that the drag torque must be sufficient to overcome the inertial torque at the output (or counter) gear to ensure rattle-free transmission. Earlier, Sakai et al. (1981) had measured the increase in rattle noise ΔL_N (in dB) for a single input and counter gear pair. The measurement indicated ΔL_N = 0 dB when $I_4\ddot{\theta}_4/T_{d4} < 1$. When $I_4\ddot{\theta}_4/T_4$ was varied from 1 to 10, ΔL_N increased by 0 to 4.6 dB. But, it should be noted that $\ddot{\theta}_4$ and $T_{d4}(t)$ are difficult to calculate when the rattle occurs. Refer to Singh et al. (1989) for more information.

C. Gear Rattle Modeling Strategies

Most models used to study the rattle problem involve a multi-degree-of-freedom lumped parameter torsional system incorporating non-linear machine elements such as a multi-stage clutch and/or backlash in one or more gear meshes. Based on our extensive experience, we have developed the following steps to successful modeling: (i) formulate a suitable model for simulation (pre-preprocessing stage), (ii) select a suitable numerical method to obtain solutions (processing stage), and (iii) choose or develop performance indices to evaluate and optimize various design parameters in order to reduce noise and vibration levels (post-processing stage). Although the study of rattle problem has been divided into three distinct stages so that various issues can be highlighted, it is clear that these stages are often inter-dependent. For instance, problems encountered in the solution stage due to numerical "stiffness" are addressed by trying to develop a suitable non-dimensionalization scheme in the pre-processing stage. Refer to Padmanabhan et al. (1995) and Singh (2007) for further details.

Generally, the numerical techniques belong to either of two categories: initial-value or boundary-value problems. A wide variety of direct time integration techniques (e.g. the many Runge-Kutta variants – Fehlberg and Verner, and others such as Gears and Adams), belong to the former, while harmonic balance and shooting methods belong to the latter. Whichever method is selected, it will be important that it be capable of successfully producing accurate time-domain results. Typical experimental validation of our computer simulation models is illustrated by Table 3.

Table 3: Experimental validation of gear rattle models

Impact Case	Gear Acceleration (peak to peak) rad/s^2	
	Theory	Experiment
None	120	104
Single-sided impacts	1550	1600
Double-sided impacts	2950	3200

8. RATTLE NOISE PERCEPTION

Of main interest is the study of the effect of various component or system designs on the vibration/shock isolation and noise perception indices with an emphasis on time domain approaches; a flowchart is given in Fig 14. Prior investigators have developed various rattle indices, some based on *intuition*, in order to evaluate the transmission design. Due to vibro-impacts, impulsive transients occur in a periodic fashion over one cycle of the acceleration time history. An increase in noise or vibration level caused by this phenomenon is a strong function of the angular acceleration peak amplitude(s) and the decay rate(s). Hence, a single measure of acceleration attenuation across the drive-train is not sufficient to characterize the system behavior. This deficiency is overcome in our proposed scheme where the excitation frequency of torque pulsations, $\omega = 2\pi/\tau$ where τ is the period, is first filtered from the predicted time histories of the acceleration signals.

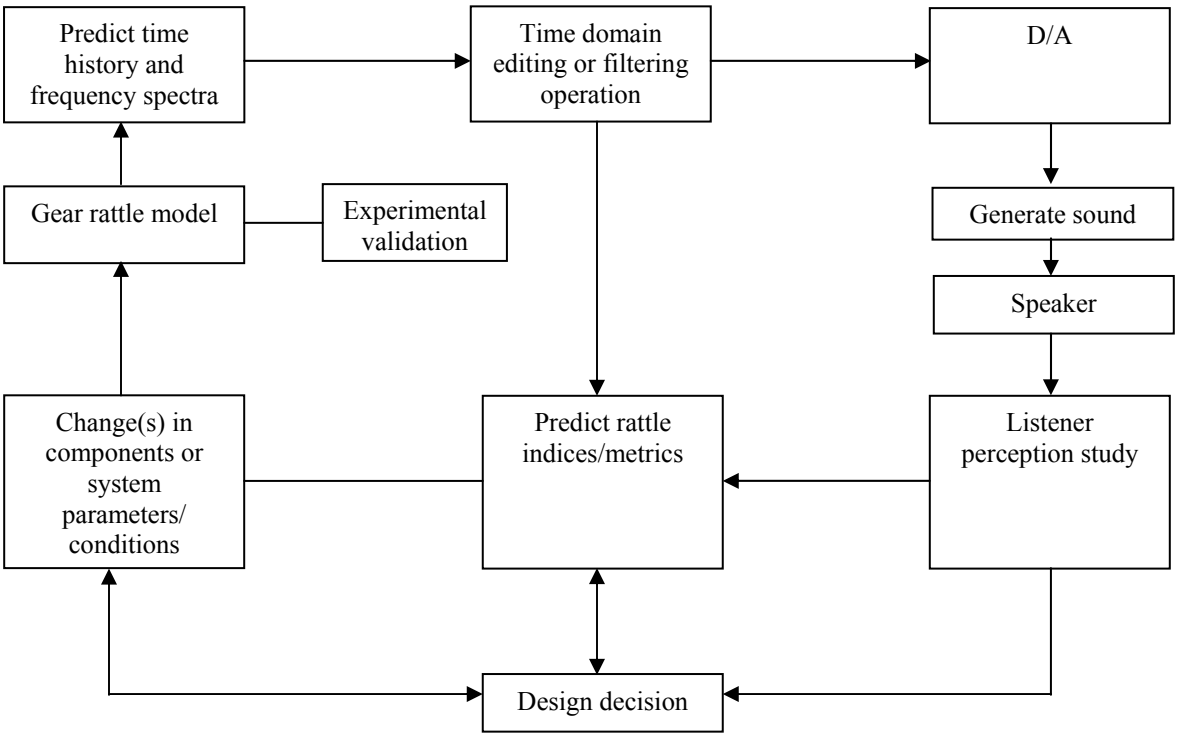

Figure 14: Flowchart of gear rattle simulation post-processing stage

Figure 15 compares the typical unfiltered and the corresponding filtered time domain accelerations of a component in the system (e.g. the gear), and one can clearly observe the characteristics of the impact transients. For instance, the impulsive transients of Fig. 15(c) show a sharp pulse followed by an exponentially decaying sinusoid. Using the unfiltered signal, two new indices, E_1 based on the ratio of mean-square values of the accelerations and E_2 based on the ratio of the peak to peak values, are developed (as defined below) to judge the effectiveness of any clutch from the noise control perspective. Further, two more indices, based on the filtered signals, are developed specifically to assess sound perception; one is based on the mean-square energy, E_3, and the other based on the energy contained within the initial sharp pulse, E_4.

$$E_1 = \left\{ \frac{\ddot{\theta}_{gear,ms}}{\ddot{\theta}_{flywheel,ms}} \right\};\ \ddot{\theta}_{i,ms} = \left\{ \frac{1}{\tau} \int_0^{\tau} \ddot{\theta}_i^2\ dt \right\};\ \tau = 2\pi/\omega; \tag{14a,b}$$

$$E_2 = \left\{ \frac{\ddot{\theta}_{gear,p}}{\ddot{\theta}_{flywheel,p}} \right\}^2;\ \ddot{\theta}_{i,p} = \left[\max\left(\ddot{\theta}_i\right) - \min\left(\ddot{\theta}_i\right) \right]; \tag{15a,b}$$

$$E_3 = \int_0^{\tau} \ddot{\theta}_{iF}^2 dt;\ E_4 = \ddot{\theta}_{iF,p}^2 \Delta t;\ \ddot{\theta}_{iF} \Rightarrow \text{Filtered}; \tag{16a,b}$$

where i ≡ torsional element index in the above equations.

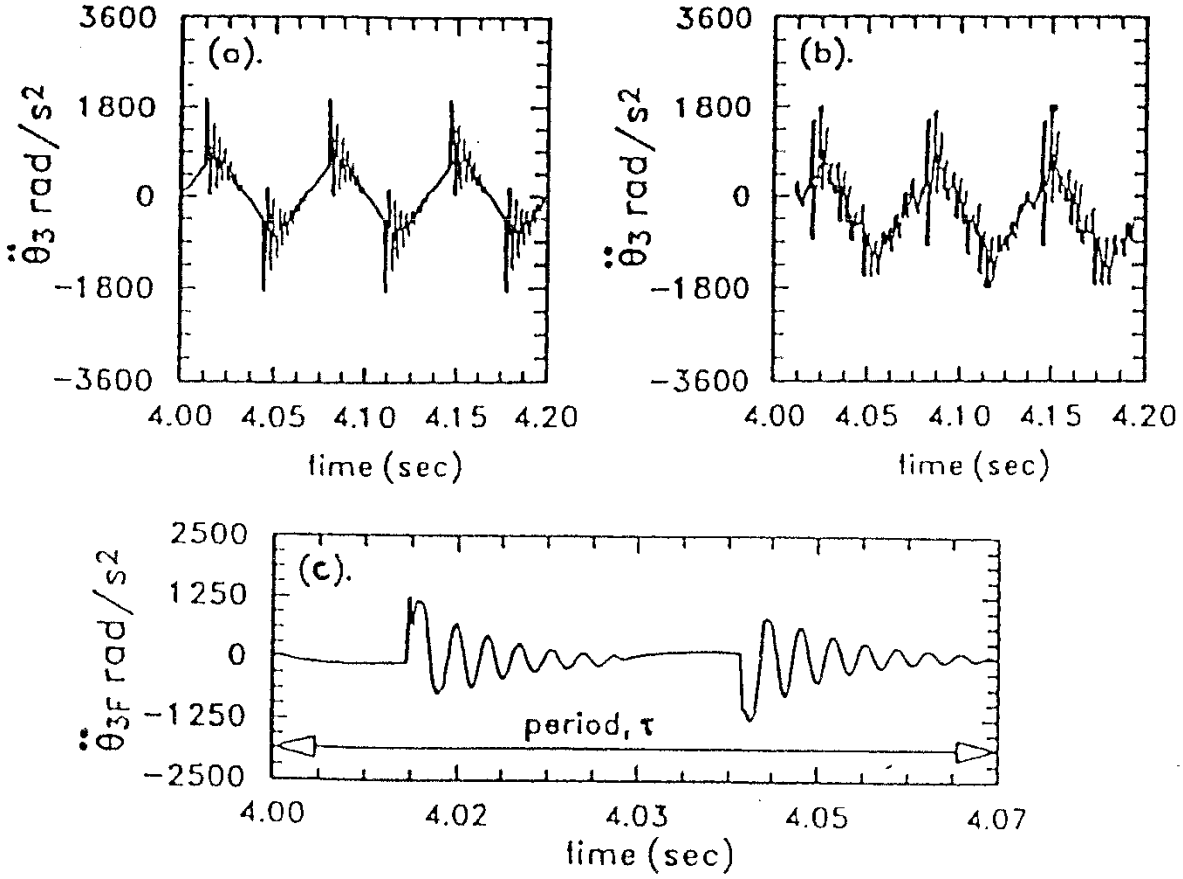

Figure 15: Typical gear rattle signatures in terms of angular acceleration time histories obtained from a. computer simulation, b. experimental measurements, and c. filtered signal shown in a.

9. RATTLE NOISE CONTROL STRATEGIES

From equations of Figures 11-13, and noting that $T_{d4} = -c_4\dot{\theta}_{m4} = c_4(R_3/R_4)\Omega_e$, the rattle criterion can now be related to R_T where R_T is torque transmissibility across the clutch damper. For the rattle-free case, the following mathematical condition is derived based on several assumptions:

$$R_T < \{(c_4\Omega_4/|T_p|)[I_1 + I_2/I_4]\}. \qquad (17)$$

Here, I_1 is the flywheel inertia, I_2 is the clutch hub inertia, I_4 is the output/input counter gear inertia, Ω_e is the engine speed, c_4 is the drag torque coefficient, T_{d4} is the drag torque (which is $c_4\Omega_e$), and $|T_p|$ is the pulsating torque. The following design solutions emerge: (i) higher drag torque on output gear (T_{d4}), or high c_4, Ω_e, (ii) very small excitation $|T_p|$, and (iii) large ($I_1 + I_2$) compared to I_4. From a typical R_T curve for a single degree of freedom linear system, one knows that $r = \omega_p/\omega_2$ should be greater than $\sqrt{2}$, and ζ_2 should be kept as low as possible. The natural frequency ω_2 can be easily altered by changing clutch stiffness k_{c1}; for low transmissibility across the clutch, k_{c1} should be as low as possible. Additionally, one can note from Equation (17) the following desirable conditions for the rattle-free case: (i) higher c_4 and engine idling

speed Ω_e to yield large T_{d4}; (ii) very small $|T_p|$ - this is intuitively obvious; and (iii) very large flywheel and clutch inertia ($I_1 + I_2$) compared to the intermediate gear I_4 – this is in agreement with experimental results (Singh, 2007). Thus one finds that Equation (17) gives several design guidelines, and is consistent with experimental and numerical findings (Singh, 2007). See Table 4 for a summary.

Table 4: Effect of vehicle transmission design trends on gear rattle

Design Change	**Parameter**	**Rattle Level or Likelihood of Rattle Occurring**
• Fewer number of engine cylinders • Diesel engines in place of gasoline engines • Turbo-charging	$\|T_p\| \uparrow$	$\uparrow$
• Reduced flywheel inertia	$I_4 \downarrow$	$\uparrow$
• Synthetic lubricants or higher temperatures	Lower viscosity	$\uparrow$
• Addition of 5^{th} speed to a 4 speed transmission	I_4 increase but T_{d4} remains the same	$\uparrow$
• High system load	$\Omega_e \downarrow$	$\uparrow$

10. CONCLUSION

Integrated models of a gearbox and its internal components are essential for accurate predictions of gear noise, and most studies on gearbox system dynamics relied on a combination of detailed finite element, boundary element and semi-analytical methods. (Gunda and Vijayakar, 2007). However, finite and boundary element methods with high resolution may require much computational time for parametric studies. In such cases, simpler models for the gearbox are more desirable.

Analytical vibro-acoustic models of a simple geared system are developed in the lecture and experimentally validated. An eight degree-of-freedom model incorporating the off-line-of-action direction is analytically formulated for a spur gear pair. Next, a model of the gearbox with embedded bearing stiffness matrices is developed to characterize the structural paths and to calculate the surface velocity distributions. Predictions are first validated by comparing with structural modal tests and transfer function measurements from gear mesh to the housing plates. Radiated noise is then estimated by using two approximate methods, namely the Rayleigh integral method and a substitute source technique. The overall vibro-acoustic model is validated by comparing radiated sound pressure calculations with measured noise data over a range of operating torques. The proposed formulation provides an efficient analytical and computational tool to quantify the relative contribution of sliding friction to the structure-borne noise, which is found to be significant when the transmission error is minimized say via tooth modifications.

Our method for computing rating indices for gear whine is based on the frequency-domain objective descriptors obtained that employ physical vibro-acoustic measurements. The proposed technique focuses on energy in narrow band frequency spectra. Implementation of this rating scheme requires several weighting functions and parameters which must be determined specifically for each product or machine considered. Once these weighting functions and parameters are found, the method provides a useful and cost effective quality rating tool which

can be used to assess various engineering changes on the reduction of objectionable gear whine during the product development phase. Further refinements in the proposed method are possible based on extensive applications to specific gear noise problems. Variations of this new rating method may be applicable to other types of quasi-steady state machinery noise problems which exhibit similar noise signatures.

This article has presented a state of the art in the modeling of transmission rattle. Specifically we have developed a step-by-step approach to address the rattle problem. Although the overall problem solving procedure is broken up into three key steps, it is essential to remember that each of these is inter-dependent on the other two steps. Current research and future plans focus on the development of new or improved semi-analytical and computational methods, impact damping mechanisms, sound perception metrics, and optimization of driveline parameters for rattle-free conditions.

Some important gear whine noise topics have not been addressed by this lecture, primarily due to space limitations. These include transmission error models and measurements, gear dynamics and resulting linear and nonlinear behavior, spectral modulations, gear blank modes, transmissibility across the bearings, casing dynamics, role of damping in controlling structure-borne noise and sound radiation, casing mounts and struts, sound radiation mechanisms, airborne sound control, failure diagnostics, and finally, active control of gear noise. Likewise, the nonlinear characterization of various torsional sub-systems that control gear rattle have not been addressed; also, a related problem (clunk) has not been covered. All of these topics are addressed by the literature cited, as well as by the basic and advanced gear noise courses that are regularly taught at the Ohio State University.

ACKNOWLEDGEMENTS

The work reported in this article is based on the efforts of many former and current students. Their contributions are gratefully acknowledged. Also, research sponsors are thanked for their financial support. Finally I would like to acknowledge Don Houser for many discussions on gear noise.

REFERENCES

Note: Only a limited set of pertinent literature (out of over 1000 publications on this topic) is cited. For instance, only a few papers on gear mechanics, gear dynamic models, and nonlinear dynamics are included. More articles can be found via the papers cited. Most of author's articles are posted on www.autonvh.org. Also, go to the www.gearlab.org for information about short courses and other materials, including a list of relevant publications.

AGMA Standard 297.02, "Sound for enclosed helical, herringbone, and spiral bevel gears," (American Gear Manufacturers Association, Alexandria, VA, 1987a).

AGMA Standard 298.01, "Sound for gearmotors and in-line reducers and increasers" (American Gear Manufacturers Association, Alexandria, VA, 1987b).

ANSI/AGMA 2000-A88, "Gear classification and inspection handbook" (American Gear Manufacturers Association, Alexandria, VA, 1988).

R. C. Barlow, C. Padmanabhan, and R. Singh, "Computational issues associated with gear rattle analysis, part II: evaluation criteria for numerical algorithms," *ASME 6th International Power Transmission and Gearing Conference, Phoenix*, 505-512 (1992).

E. Baron, B. Favre, and P. Mairesse, "Analysis of relation between gear noise and transmission error," INTER-NOISE 1988 **2**, 611-614 (1988).

G.W. Blankenship and R. Singh, "Development of a signal processing technique for the objective rating of gear noise," *Noise Control Eng. J.* **38**(2), 81-92 (1992a).

G.W. Blankenship and R. Singh, "A comparative study of selected gear mesh force interface dynamic models," ASME 6th Int. Power Transmission and Gearing Conference, Phoenix, *DE-43-1*, 137-146 (1992b).

G. W. Blankenship and R. Singh, "Analytical solution for modulation side bands associated with a class of mechanical oscillators," *J. Sound Vib.* **179**(1), 13-36 (1995a).

G. W. Blankenship and R. Singh, "A new gear mesh interface dynamic model to predict multi-dimensional force coupling and excitation," *Mechanism and Machine Theory Journal* **30**(1), 43-57 (1995b).

J. Börner and D. R. Houser, "Influence of friction and bending moments on gear noise excitations," SAE, Paper # 961816 (1996).

E. Buckingham, *Analytical Mechanics of Gears* (Dover, 1949).

C. Chung, G. Steyer, T. Abe, M. Clapper, and C. Shah, "Gear noise reduction through transmission error control and gear blank dynamic tuning," SAE, Paper # 1999-01-1766 (1999).

R. J. Comparin and R. Singh, "An analytical study of automotive neutral gear rattle," *ASME J. of Mech. Design* **112** (June), 237-245 (1990).

A. R. Crowther, C. Janello and R. Singh, "Quantification of clearance-induced impulsive sources in a torsional system," *J. Sound Vib*, **307**, 428-451 (2007a).

A. R. Crowther, R. Singh, N. Zhang and C. Chapman, "Impulsive response of an automatic transmission system with multiple clearances: formulation, simulation and experiment," *J. Sound Vib* **306**, 444-466 (2007b).

R. J. Drago, "Minimizing noise in transmissions," *Machine Design*, January, 143-148 (1981).

R. Drago, J. Lenski, R. Spencer, M. Valco, and F. B. Oswald, "The relative noise levels of parallel axis gear sets with various contact ratios and gear tooth forms" AGMA Fall Technical Meeting, Paper 93FTM11 (1993).

T. Fujimoto, Y. Chikatani, and J. Kojima, "Reduction of idling rattle in manual transmission," SAE, Paper # 870395 (1987).

C. George, "Gear Noise Sources and Controls," in *Reduction of Machinery Noise*, edited by M. J. Crocker (Purdue University, 1974).

R. W. Gregory, S. L. Harris, and R. G. Munro, "Dynamic behavior of spur gears," *Proc. I. Mech. E.* **178**(8), 207-226 (1963-4).

R. Gunda and S. Vijayakar, "Application of the Fast Multipole Method (FMM) for acoustic analysis," NOISE-CON 2007, Paper #196 (2007). [COUSTYX code is available from www.ansol.com]

J. S. Gurm, W. J. Chen, A. Keyvanmanesh, T. Abe, A. R. Crowther and R. Singh, "Transient clunk response of a driveline system: laboratory experiment and analytical studies," *SAE Trans. J. Passenger Cars: Mechanical Systems* **V116-6**, Paper # 2007-01-2233 (2008).

S. He, R. Gunda and R. Singh, "Effect of sliding friction on the dynamics of spur gear pair with realistic time-varying stiffness," *J. Sound Vib.* **301**, 927-949 (2007).

S. He, S. Cho and R. Singh, "Prediction of dynamic friction forces in spur gears using alternate sliding friction formulations," *J. Sound Vib.* **309**(3-5), 843-851 (2008a).

S. He, R. Singh and G. Pavic, "Effect of sliding friction on gear noise based on a refined vibro-acoustic formulation," *Noise Control Engineering Journal* **56**(3), 164-175 (2008b).

D. R. Houser, "Gear noise sources and their prediction using mathematical models," Chap. 16 in *Gear Design Manufacturing and Inspection Manual* (SAE, Warrendale, PA, 1990).

D. R. Houser, "Gear Noise," Chap. 14 in *Dudley's Gear Handbook*, edited by D. Townsend (McGraw Hill, New York, 1992).

D. R. Houser, "Gear Noise and Vibration Prediction and Control Methods," Chap. 69 in *Handbook of Noise and Vibration Control*, edited by M. J. Crocker (John Wiley, 2007).

D. R. Houser and J. Harianto, *Load Distribution Program Reference Manual*, (GearLab, The Ohio State University, Columbus, Ohio, 2009)

D. R. Houser, and R. Singh, *Basic Gear Noise Short Course Notes* (The Ohio State University, 2008).

D. R. Houser, M. Vaishya and J. D. Sorenson, "Vibro-acoustic effects of friction in gears: an experimental investigation," SAE, Paper # 2001- 01-1516 (2001).

M. F. Jacobson, R. Singh and F. B. Oswald, "Acoustic radiation efficiency models of a simple gearbox," ASME 7th Int. Power Transmission and Gearing Conference, *DE 88*, 597–601 (1996).

A. Kahraman and R. Singh, "Interactions between time-varying mesh stiffness and clearance nonlinearity in a gear system," *J. Sound Vib.* **146**(1), 135-156 (1991).

V. Kartik and D. R. Houser, "An investigation of shaft dynamic effects on gear vibration and noise excitations," *SAE Transactions, J. Passenger Car Mech. Syst.* **112**, 1737-1746 (2003).

S. Kim and R. Singh, "Gear surface roughness induced noise prediction based on a linear time-varying model with sliding friction," *J. Vib. Control* **13**(7), 1045-1063 (2007).

T. C. Kim and R. Singh, "Dynamic interactions between loaded and unloaded gear pairs under rattle conditions," *SAE Trans. J. Passenger Cars: Mechanical Systems*, **110**, 1934-1943 (2002).

T. C. Kim, T.E. Rook and R. Singh, "Effect of smoothening functions on the frequency response of an oscillator with clearance non-linearity," *J. Sound Vib.* **263**(3), 665-678 (2003).

T. C. Kim, T.E. Rook and R. Singh, "Effect of impact damping on the frequency response characteristics of a torsional system," *J. Sound Vib.* **281**(3-5), 995-1021 (2005a).

T. C. Kim, T.E. Rook and R. Singh, "Super- and sub-harmonic response calculations for a torsional system with clearance non-linearity using harmonic balance method," *J. Sound Vib.* **281**(3-5), 965-993 (2005b)

T. C. Lim and R. Singh, "A review of gear housing dynamics and acoustics literature," NASA-Technical Memorandum, 89-C-009 (1989).

T. C. Lim and R. Singh, "Vibration transmission through rolling element bearings. Part I: bearing stiffness formulation," *J. Sound Vib.* **139**(2), 179-199 (1990a).

T. C. Lim and R. Singh, "Vibration transmission through rolling element bearings. Part II: system studies," *J. Sound Vib.* **139**(2), 201-225 (1990b).

T. C. Lim and R. Singh, "Statistical energy analysis of a gearbox with emphasis on the bearing path," *Noise Control Eng. J.* **37**(2), 63-69 (1991a).

T.C. Lim and R. Singh, "Vibration transmission through rolling element bearings. Part III: geared systems studies," *J. Sound Vib.* **151**(1), 31-54 (1991b).

T.C. Lim and R. Singh, "Vibration transmission through rolling element bearings. Part IV: statistical energy analysis," *J. Sound Vib.* **153**(1), 37-50 (1992).

T.C. Lim and R. Singh, "Vibration transmission through rolling element bearings, Part V: effect of distributed contact load on roller bearing stiffness matrix," *J. Sound Vib.* **169**(4), 547-553 (1994).

W. D. Mark, “Contributions to the vibratory excitation of gear systems from periodic undulation on tooth running surfaces,” *J. Acoust. Soc. Am.* **91**(1), 166-186 (1992a).

W. D. Mark, “Elements of Gear Noise Prediction,” Chap. 21 in *Noise and Vibration Control Engineering*, edited by L. L. Beranek and I. Ver (John Wiley, 1992b).

L. D. Mitchell, “Gear noise: the purchaser’s and the manufacturer’s view,” *Proc. of the Purdue Noise Control Conference*, pp. 95-106 (1971).

P. J. Mucci and R. Singh, “Active vibration control of a beam subjected to AM or FM disturbances,” *Noise Control Eng. J.* **43**(5), 159-171 (1995).

R. G. Munro, “A review of the theory and measurement of gear transmission error,” *Gearbox Noise and Vibration Proc., I. Mech. E.* (Cambridge, UK, 1990).

G. Niemann and J. Baethge, “Transmission error, tooth stiffness and noise of spur and helical gears – part 1,” Vol. 112 (Drehwegfehler, Zahnfederharte und Gerausch bei Stirnradern, VDIZ, 1970).

S. Ohnuma, Y. Shigetaro, I. Mineichi, and T. Fujimoto, “Research on idling rattle of manual transmission,” SAE, Paper # 850979 (1985).

H. Opitz, “Noise of gears,” *Phil. Trans. R. Soc.* **263** (December) 369-380 (1972).

H. N. Özguven and D. R. Houser, “Mathematical models used in gear dynamics - a review,” *J. Sound Vib.* **121**(3), 383-411 (1988).

C. Padmanabhan and R. Singh, “Influence of clutch design on the reduction and perception of automotive rattle noise,” *NOISE-CON 93*, 607-612 (1993).

C. Padmanabhan and R. Singh, “Analysis of periodically forced non-linear hills oscillator with application to a geared system,” *J. Acoustical Soc. America* **99**(1), 324-334 (1996).

C. Padmanabhan, R. C. Barlow, T. E. Rook, and R. Singh, “Computational issues associated with gear rattle,” *ASME J. Mech. Design* **117**, 185-192 (1995).

G. Pavić, “An engineering technique for the computation of sound radiation by vibrating bodies using substitute sources,” *J. Acta Acustica* **91**, 1-16 (2005).

G. Pavić, “A technique for the computation of sound radiation by vibrating bodies using multipole substitute sources,” *Acta Acustica Journal* **92**, 112-126 (2006).

T. E. Rook and R. Singh, “Dynamic analysis of a reverse-idler gear pair with concurrent clearances,” *J. Sound Vibr.* **182**(2), 303-322 (1995).

T. E. Rook and R. Singh, "Mobility analysis of structure-borne noise power flow through bearings in gearbox-like structures," *Noise Control Eng. J.* **44**(2), 69-78 (1996).

T. E. Rook and R. Singh, "Structural intensity calculations for compliant plate-beam structures connected by bearings," *J. Sound Vib.* **211**(3), 365-388 (1998).

A. Van Roosmalen, "Design tools for low noise gear transmissions," Ph.D. Dissertation, Eindhoven University of Technology (1994).

T. Sakai, Y. Doi, M. Yamamoto, T. Ogasawara, and M. Narita, "Theoretical and experimental analysis of rattling noise of automotive gearbox," SAE, Paper # 810773 (1981).

R. Singh, "Dynamic design of powertrains for reduced vibro-impacts" in *Optimum Dynamic Design*, pp. 305-317 (Allied Publishers, 1997).

R. Singh, *Advanced Gear Noise Short Course Notes: Gear Rattle* (The Ohio State University, 2007).

R. Singh, H. Xie, and R. Comparin, "Analysis of automotive neutral gear rattle," *J. Sound Vib.* **131**(2) 177-196 (1989).

R. Singh, A. Lake, V. Asnani and S. He, "Vibro-acoustic model of a geared system including friction excitation," INTER-NOISE 2007, Paper # 663296, 28-31 (2007).

J. D. Smith, *Gear Noise and Vibration* (Marcel Dekker, New York and Basel, 1999)

G. Steyer, "Influence of gear train dynamics on gear noise," NOISE-CON 87 Proc., 53-58 (1987).

J. I. Taylor, *The Gear Analysis Handbook* (Vibration Consultants, Tampa Bay, Florida, 2000).

J. Tuma, "Transmission and Gearbox Noise and Vibration Prediction and Control," Chap. 88 in *Handbook of Noise and Vibration Control*, edited by M. J. Crocker (John Wiley, 2007).

M. Vaishya and R. Singh, "Strategies for modeling friction in gear dynamics," *ASME J. Mech. Design* **125**, 383-393 (2003).

H. Vinayak and R. Singh, "Dynamic analysis of flexible gears for high power density transmissions," *International Gearing Conference*, 105-110 (Newcastle, UK, 1994).

H. Vinayak, R. Singh, and C. Padmanabhan, "Linear dynamic analysis of multi-mesh transmissions containing external, rigid gears," *J. Sound Vib.* **185**(1), 1-32 (1995).

D. B. Welbourn, "Fundamental knowledge of gear noise – a survey," *Proc. Noise Vib. Eng. Trans., I. Mech E.*, **14**, 9-14 (1979).